

Electromodulation of the electronic structure and optical properties of [111]-growth-axis superlattices

C. Mailhot

Xerox Webster Research Center, 800 Phillips Road, 0114-41D, Webster, New York 14580

D. L. Smith

Los Alamos National Laboratory, Los Alamos, New Mexico 87545

(Received 22 February 1988)

We show that large, linear electrooptic coefficients are expected in strained-layer superlattices grown along the [111] axis. The linear electrooptic effects in these superlattices are due to the large, piezoelectrically generated internal electric fields which occur in them. Such linear electrooptic coefficients are not expected in lattice matched superlattices or superlattices grown along [100].

Materials whose optical properties can be modulated by application of an external electric field are valuable in the area of optoelectronics. However, the magnitude of the index-of-refraction modulation that can be achieved in conventional electrooptic materials is rather small. Recently, there has been considerable interest in the electrooptic properties of superlattices because rather large second-order electrooptic coefficients occur in these materials.¹⁻⁶ In this Rapid Communication, we predict very large first-order electrooptic coefficients in strained-layer superlattices grown along the [111] crystallographic axis.

It is now well established that strained-layer superlattices can be grown with a high degree of crystalline perfection.⁷⁻⁹ For sufficiently thin layers, the lattice-constant mismatch is accommodated by internal strains rather than by the formation of dislocations. Group III-V and group II-VI semiconductors are piezoelectric. Thus, strains in these materials can lead to electric polarization fields. For strained-layer superlattices with a [111] growth axis, the orientation of the lattice-constant mismatch-induced strains is such that polarization fields directed along the growth axis are generated.^{10,11} Because one of the constituent materials is in biaxial compression, and the other is in biaxial tension, the signs of the electric polarization vectors are opposite in the two constituent materials. Thus, there is a nonzero divergence of polarization (a polarization charge) at the superlattice interfaces. These polarization charges generate internal electric fields directed along the growth axis and having opposite polarities in the two constituent materials. The magnitude of the electric fields can be very large, exceeding 10^5 V/cm, for lattice-constant mismatches of the order of 1%.

The strain-induced electric fields can significantly change the electronic structure and the optical properties of the superlattice.^{12,13} For example, they change electronic energy levels and wave functions, and thus optical transition energies and oscillator strengths. As is usual with the Stark effect, these changes are second order in the magnitude of the electric field. The internal, strain-induced electric fields can be modulated by application of an external electric field. The external field will be essentially uniform whereas the internal electric field reverses

polarity in the two constituent materials. Thus the total electric field is increased in one constituent material type and decreased in the other. In type-I superlattices, the magnitude of the electric field in the quantum wells is much more important than in the barriers. If the magnitude of the external field is small compared with that of the internal field, changes in the superlattice electronic structure and optical properties due to the external field will be linear in the magnitude of the external field. This situation corresponds to a second-order effect (Stark effect) being modulated by the applied field about a large bias point due to the strain generated internal fields. As a result, a linear electrooptic effect is expected in [111] growth-axis strained layer superlattices which have large internal electric fields whereas a quadratic electrooptic effect is expected in [100] growth-axis superlattices and in [111] growth-axis lattice-matched superlattices which do not have those internal electric fields.

We consider lattice-matched $\text{Ga}_{0.47}\text{In}_{0.53}\text{As}-\text{Al}_{0.48}\text{In}_{0.52}\text{As}$ and strained-layer $\text{Ga}_{0.47}\text{In}_{0.53}\text{As}-\text{Al}_{0.7}\text{In}_{0.3}\text{As}$ superlattices grown along the [111] axis. The strained-layer superlattice has the internal electric fields and the lattice-matched superlattice does not. A [100] growth-axis superlattice (strained-layer or lattice-matched) would not have internal fields and would be qualitatively similar to the lattice-matched [111] case. We consider superlattices in which the Ga-containing alloy layers are half as thick as the Al-alloy layers. Both the lattice-matched and strained-layer case are type-I superlattices in which the Ga alloy is the quantum well. For the strained-layer case, the quantum well is in biaxial compression with a lattice-constant mismatch of 1.5%. The strain-induced electric field is 1.4×10^5 V/cm in the Ga alloy and half this value in the Al alloy. We have previously presented electronic structure and optical properties calculations for these superlattices without an external electric field.^{12,13} We use the same calculational approach¹⁴ and input parameters here. For calculational simplicity, we approximate the total electric field by a field which produces a periodic potential. The internal field alone has this property, but the smaller external field breaks up the periodicity. The field in the quantum well is correctly treated. The field in the

barrier is adjusted to give the periodic potential. This approximation is appropriate for type-I superlattices in which there is essentially no coupling between quantum wells. This is the case considered here. The approximation is not justified for type-I superlattices in which there is significant coupling between quantum wells. Analogous approximations would not be justified in type-II superlattices.

In Fig. 1, the variation of the HH_1-C_1 transition energy at the center of the superlattice Brillouin zone is shown as a function of the magnitude of the externally applied electric field. (Here HH and C refer to heavy-hole and conduction subbands, respectively.) The external electric field is applied along the $[111]$ growth axis and has the same sign as the internal field in the Ga alloy quantum well. Results are shown for various layer thicknesses. For the lattice-matched superlattice, the external field decreases the transition energy. The effect is larger for thicker layer superlattices. The decrease in transition energy is essentially quadratic with the magnitude of the applied field. The sign of the applied field is not important for the lattice-matched superlattice. For the strained-layer superlattice, the external field adds to the strain-induced electric field in the quantum well and decreases the transition energy. The effect is larger for thicker-layer superlattices. The decrease in transition energy is essentially linear with the magnitude of the applied field and is much larger than for the lattice-matched superlattice. The sign of the applied field is important for the strained

layer superlattice; for the opposite polarity to that in Fig. 1, the transitions will shift to higher energy.

In Fig. 2, the variation of HH_2-C_1 transition energy is shown. For the lattice-matched superlattice, this transition energy shows a complex nonlinear behavior due to mixing of heavy-hole states by the applied field. For the strained-layer superlattice, the strain-generated electric field separates the heavy-hole state energies. The change in transition energy due to the external field is essentially linear for the range of fields considered.

In Fig. 3, we show the absorption coefficient and the resonant contribution to the real part of the refractive index as a function of photon energy for strained-layer and lattice-matched superlattices with 25 molecular layers of the Ga alloy and 50 molecular layers of the Al alloy. Results are shown with no applied electric field and with a 40-kV/cm applied electric field. Transitions from the first two heavy-hole bands to the lowest conduction band are included. (Other transitions occur outside of the energy range shown.) Exciton effects are included in these optical calculations. A scattering time (T_2), which gives a full width at half maximum of 6 meV, was used. For the lattice-matched superlattice, the HH_1-C_1 transition strongly dominates the spectra with no applied field. (The HH_2-C_1 transition is very weak in this case.) As the external field is applied, the HH_1-C_1 transition moves to lower energy and loses oscillator strength whereas the HH_2-C_1 transition stays approximately constant in energy and gains oscillator strength. For the strained-layer superlattice, the HH_1-C_1 and HH_2-C_1 transitions are both fairly strong with no applied field. The internal field has caused the HH_2-C_1 transition to be strongly allowed.

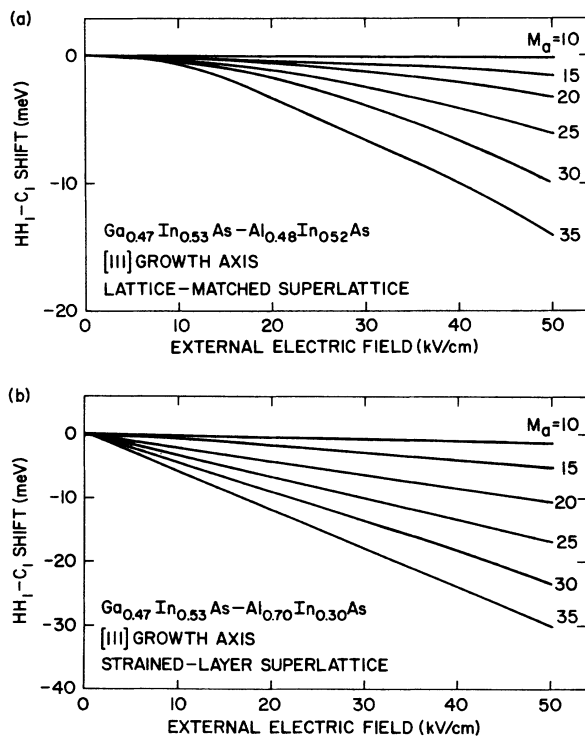


FIG. 1. Variation of the HH_1-C_1 transition energy as a function of the magnitude of the applied field for $Ga_{1-x}In_xAs-Al_{1-y}In_yAs$ superlattices grown along the $[111]$ axis. The superlattice consists of M_a layers of $Ga_{1-x}In_xAs$ (wells) alternating with $M_b = 2M_a$ layers of $Al_{1-y}In_yAs$ (barriers).

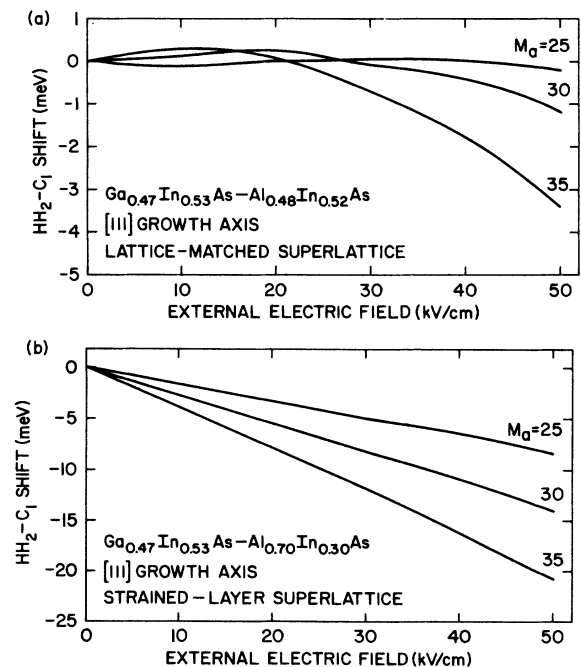


FIG. 2. Variation of the HH_2-C_1 transition energy as a function of the magnitude of the applied electric field for $Ga_{1-x}In_xAs-Al_{1-y}In_yAs$ superlattices grown along the $[111]$ axis.

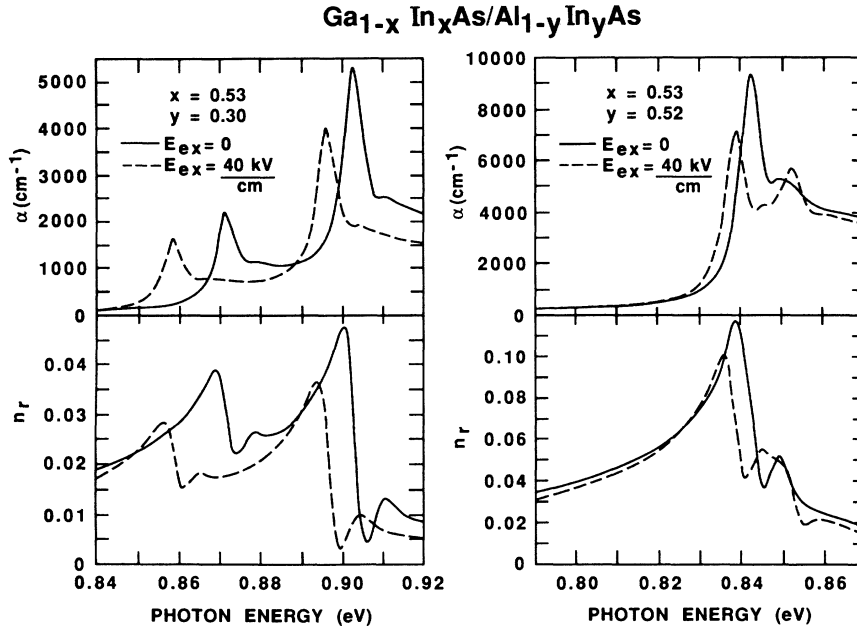


FIG. 3. Absorption coefficient and resonant part of the refractive index with and without an applied electric field as a function of photon energy for $M_a = 25$; $M_b = 50$ strained-layer and lattice-matched superlattices.

Indeed, it is even stronger than the HH_1-C_1 transition. As the external field is applied (the applied electric field has the same sign as the internal field in the Ga-alloy quantum well), both the HH_1-C_1 and HH_2-C_1 transitions move to lower energy. The shift is larger for the HH_1-C_1 transition. Both transitions lose oscillator strength which goes to higher energy transitions.

In Fig. 4 we show calculated electrooptic coefficients for the strained-layer superlattice described above. The

coefficient r is defined by

$$n(E) - n(0) = - \frac{|n(0)|^3 r E}{2}, \quad (1)$$

where n is the index of refraction and E is the applied field. The index of refraction calculations in Fig. 3 were used to construct the electrooptic coefficients presented in Fig. 4. The total index of refraction which appears in Eq. (1) consists of the field-dependent, resonant part shown in

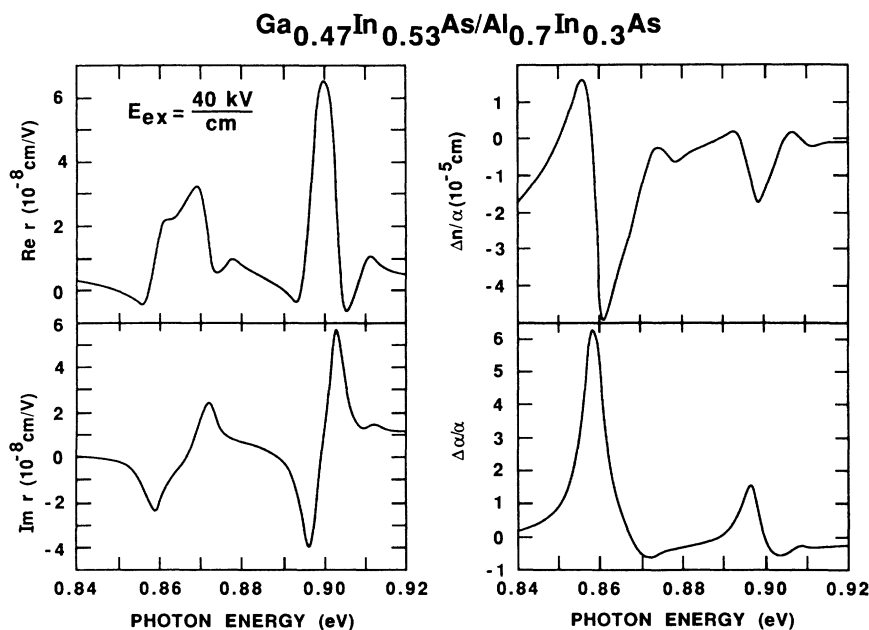


FIG. 4. Electrooptic coefficients as a function of photon energy for the $M_a = 25$; $M_b = 50$ strained-layer superlattice.

Fig. 3 plus a field-independent, nonresonant part. We get the nonresonant part by averaging the nonresonant indices of refraction of the superlattice constituent materials. For many electrooptic applications, the change in refractive index or absorption coefficient divided by the zero-field absorption coefficient is an important figure of merit. Therefore, in Fig. 4, we also show

$$\Delta n/\alpha = \frac{n(E) - n(0)}{\alpha(0)},$$

and

$$\Delta\alpha/\alpha = \frac{\alpha(E) - \alpha(0)}{\alpha(0)},$$

for $E = 40$ kV/cm as a function of photon energy. The coefficients plotted in Fig. 4 attain very large values. For comparison, in potassium dihydrogen phosphate, the coefficient r is about 10^{-9} cm/V.¹⁵

In conclusion, we have predicted that large linear electrooptic coefficients will occur in [111] strained layer superlattices because of the internal, piezoelectrically generated electric fields in these superlattices.

The work of one of us (D.L.S.) has been financially supported by the Los Alamos National Laboratory Internal Supporting Research.

- ¹D. A. B. Miller, D. S. Chemla, T. C. Damen, A. C. Gossard, W. Wiegmann, T. H. Wood, and C. A. Burrus, *Phys. Rev. Lett.* **53**, 2173 (1984); *Phys. Rev. B* **32**, 1043 (1985).
²D. A. B. Miller, D. S. Chemla, T. C. Damen, T. H. Wood, C. A. Burrus, A. C. Gossard, and W. Wiegmann, *IEEE J. Quantum Electron.* **QE-21**, 1462 (1985).
³D. A. B. Miller, D. S. Chemla, and S. Schmitt-Rink, *Phys. Rev. B* **33**, 6976 (1986).
⁴T. H. Wood, R. W. Tkach, and A. R. Chraplyvy, *Appl. Phys. Lett.* **50**, 798 (1987).
⁵H. Yamamoto, H. Asada, and Y. Suematsu, *Electron. Lett.* **21**, 579 (1985).
⁶Y. C. Chang, J. N. Schulman, and U. Efron, *J. Appl. Phys.* **62**, 4533 (1987).
⁷J. W. Matthews and A. E. Blakeslee, *J. Cryst. Growth* **27**, 118 (1974); **29**, 273 (1975); **32**, 265 (1976).

- ⁸G. C. Osbourn, R. M. Biefield, and P. L. Gourley, *Appl. Phys. Lett.* **41**, 172 (1982).
⁹I. J. Fritz, L. R. Dawson, and T. E. Zipperian, *Appl. Phys. Lett.* **43**, 846 (1983).
¹⁰D. L. Smith, *Solid State Commun.* **57**, 919 (1986).
¹¹For strained-layer superlattices with growth axis along [100], no polarization fields are generated.
¹²C. Mailhiot and D. L. Smith, *Phys. Rev. B* **35**, 1242 (1987).
¹³D. L. Smith and C. Mailhiot, *Phys. Rev. Lett.* **58**, 1264 (1987).
¹⁴D. L. Smith and C. Mailhiot, *Phys. Rev. B* **33**, 8345 (1986); C. Mailhiot and D. L. Smith, *Phys. Rev. B* **33**, 8360 (1986).
¹⁵I. P. Kaminow and E. H. Turner, in *Handbook of Lasers*, edited by R. J. Pressley (The Chemical Rubber Co., Cleveland, 1971), p. 452.